Annals of Phytomedicine 13(1): 1100-1110, 2024

DOI: http://dx.doi.org/10.54085/ap.2024.13.1.118

Annals of Phytomedicine: An International Journal
http://www.ukaazpublications.com/publications/index.php

Print ISSN : 2278-9839 Online ISSN : 2393-9885

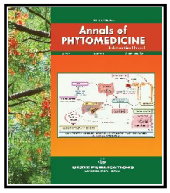

Original Article : Open Access

Isolation and characterization of α-glucosidase inhibitors from *Phyllanthus acidus* (L.) Skeels stem bark

Zeba Siddiqui, Mohammad Irfan Khan◆, Badruddeen, Juber Akhtar, Mohammad Ahmad, Manvi and Gayyur Fatima
Faculty of Pharmacy, Integral University, Lucknow-226026, Uttar Pradesh, India

Article Info

Article history
Received 4 January 2024
Revised 23 February 2024
Accepted 24 February 2024
Published Online 30 June 2024

Keywords
Isolation
Chromatography
Spectroscopy
α-glucosidase inhibitor
Diabetes

Abstract

In our quest for potential α-glucosidase inhibitors with an objective to develop novel therapeutics for the management and treatment of diabetes and related disorders; three phytoconstituents were isolated from the stem bark of *Phyllanthus acidus* (L.) Skeels. These compounds were elucidated by both phytochemical and spectroscopic analysis. Of the isolated compounds, one was an aliphatic hydrocarbon, a sterol and a pentacyclic triterpenes. All these phytoconstituents, *i.e.*, n-docosane, β-sitosterol and lupeol although have been reported previously but have been isolated from stem bark of *P. acidus* for the first time, to the best of our knowledge. Among the isolated compounds, β-sitosterol and lupeol showed considerable α-glucosidase inhibitor activity comparable to that of antidiabetic drug acarbose, and therefore chloroform extract of *P. acidus* deserve further development as potential new drugs for diabetes.

1. Introduction

Diabetes mellitus (DM) has become one of the most frequently occurring metabolic disorders with considerable mortality and morbidity and has become a cause of widespread concern around the world due to severe and high rate of incidence (ADA, 2014; Ogurtsova *et al.,* 2017; Ajmal *et al.,* 2023). Over the past few decades, the occurrence of diabetes has increased expeditiously with more than 400 million people suffering from diabetes around the world .The number is expected to rise to 642 million over the next twenty years. Due to sedentary lifestyle, the incidence of diabetes in younger generation especially obese children before puberty is also growing and a cause of concern in both developed and developing nations (Zhou *et al.*, 2016). Hyperglycaemia over a protracted period of time may result in a numerous serious complications like stroke, diabetic neuropathy, foot ulcers, neuropathy, nephropathy and many more (Singh *et al.*,2023; Marcovecchio *et al.,* 2011). Progression of the disease also results in delayed wound healing process (Palai *et al.*, 2023; Kumari *et al.,* 2023). However, the control of postprandial hyperglycemia is paramount in initial stages of diabetes therapy (Lebovitz, 2001). Among the various approaches adopted for the management of postprandial hyperglycemia one is to retard absorption of glucose by repression of carbohydrate-hydrolyzing enzyme like, α-amylase and α-glucosidase, present in the digestive system (Toeller, 1994). For their catalytic role in the hydrolysis of glycosidic linkage of terminal glucose at the cleavage site α-glucosidase inhibitors has been of keen interest not only to pharmaceutical industry but also as therapeutic target for the various diseases involving carbohydrate modulation like hepatitis, cancer, cardiovascular diseases and viral infections (Mehta *et al.,* 1998; Zitzmann *et al.,* 1999). Following the discovery of the first α-glucosidase inhibitor acarbose which have been approved for the management of type 2 diabetes, various other á-glucosidase inhibitors have been discovered and explored extensively for the treatment of hypoglycaemia (Yee and Fong, 1996). They include novel synthetic molecules, compounds obtained from natural resources as well as transition state analogues (Gao and Kawabata, 2008; Seo *et al.,* 2005). Another approach for the management of diabetes and related complications is the scavenging of free radicals like reactive oxygen species obtained due to oxidative stress which overrides the antioxidant ability of the cellular organisation resulting in cell damage (Duraisami *et al.,* 2021). Excess of superoxide produced in mitochondria is one of the main causes of diabetes related tissue damage, destruction of β-cells and insulin resistance which may lead to compromised glucose tolerance (Liu *et al.,* 2007). Detrimental outcomes of this effect have been responsible for the secondary complications in diabetes mellitus. Thus, another approach to manage and palliate the effect of these free radicals may be *via* the use of antioxidants that have been experimentally proven to reduce the destruction of β-cells of pancreas by halting auto-oxidation chain reaction, thereby halting the progression of complications associated with diabetes (Sabiu *et al.,* 2016). Therefore, the antioxidant potential of *P. acidus* stem bark has been researched and reported by us in our previous studies (Siddiqui *et al.,* 2022). However, the carcinogenicity associated with synthetic antioxidants has resolved in search of plant based antioxidants that have lower toxicity incidents (Aslan *et al.,* 2010).

The genus *Phyllanthus* is part of one of the enormous genus in the Phyllanthaceae family and has about 1000 species. The species are well distributed throughout the world mainly in tropics and sub-tropical regions. Many of them are reported to possess a variety of medicinal activities. Some of the well known plants of this genus like

Corresponding author: Dr. Mohammad Irfan Khan
Associate Professor, Faculty of Pharmacy, Integral University, Lucknow-226026, Uttar Pradesh, India
E-mail: irfan9896@gmail.com
Tel.: +91-7897124030

Phyllanthus emblica (Indian Gooseberry, Amla) and *Phyllanthus amarus* (Bhui amla, niruri) have well documented uses in Ayurveda, Siddha, Unani, Arabic, Tibetan and Egyptian texts (Unander *et al*., 1990). One of the members of this genus is an decorative plant with elaborate history of folklore and culinary applications. Othaheite gooseberry, *i.e., Phyllanthus acidus* has yellow greenish fruits that do not look like Indian gooseberry other than for the sourness of their fruits. The plant that is considered to have its origin in Madagascar is now mostly grown in India and Malay Peninsula (Morton, 1987). The fruit is slightly bitter, fragrant, acrid, and acidic and improves hunger. In Indian Traditional system, it is applied for the management of lung infections, piles and biliousness. The fruit is utilized as tonic for liver and blood (Hazarika *et al*., 2012). Latex is said to have nauseating and cathartic activity. Its bark is warmed with coconut oil and applied on boils on feet and hands. Roots are used for the cure of psoriasis while its infusion is used for the treatment of asthma and for curing headache and cough (Lemmens, 1999). Mucilage from the leaves is applied as demulcent for cure of gonorrhea (Rizk, 1987). An overview of the published literature indicated that the plant is mainly rich in phenols, terpenoids, flavonoid and volatile oils (Tan *et al.,* 2020). Various parts of *P. acidus* have been studied for various pharmacological activities. The roots and fruits of *P. acidus* has been found to possess effective antidiabetic activity (Siddiqui *et al.,* 2022).

2. Materials and Methods

2.1 Chemicals and instruments

Chemicals of analytical grade and reagents were procured from SD Fine Ltd. All the solvents used in column chromatography were first dried using a drying agent (Sodium sulphate). Weighing was done by the use single pan mettler scale. Ultra-violet spectra were recorded on Hitachi 150-20 spectrophotometer. Infrared spectra were documented in potassium bromide disc on FTIR Perkin Elmer spectrometer, λ_{max} values were stated in centimeter$^{-1.}$ Protons ^{1}H-NMR spectrum were recorded on, 400 MHz, Brucker Spectrospin utilizing $CDCl_3$ and DMSO solvents and internal standard used was TMS. Chemical shift readings were stated as δ (ppm) scale and coupling constant (J) expressed in Hz. The spin-coupled pattern is assigned as: singlet (s), doublet (d), double (dd), triplet (t), multiplet (m), and unreserved broad signal (br). The ^{13}C-NMR spectrums were documented on 400 MHz nuclear magnetic resonance (NMR) spectrometer at 27°C. The HRMS were documented on a liquid chromatography/orbitrap mass spectrometer.

2.2 Plant collection and authentication

The dried stem barks of *P. acidus* were collected from Valara forest in Iduki district, Kerala. The collected samples were authenticated with deposited specimens by Dr. K. M. Prabhukumar, Senior Scientist and Herbarium Curator, at the National Botanical Research Institute, Lucknow, India (PDSH/LWG/Authentication/2022-23/04).

2.3 Extraction and fractionation

The *P. acidus* stem barks was dried in air, in shade and pulverized in an automatic grinder. The powdered stem bark (1.5 kg) was extracted exhaustively with 2 l of methanol in Soxlet assembly for 72 h, at moderate temperature. The extract was then filtered under vacuum and concentrated with the help of rotary evaporator to yield 140 g of solid brown extract of *P. acidus*.

The 40 g of crude extract was separately fractionated on silica gel (mesh size 60-120), packed column, and eluted with petroleum ether, chloroform and ethanol, respectively, to obtain petroleum ether, chloroform and ethanolic fractions, respectively. The fractions were vaporized and stored at –20°C for further pharmacological studies.

2.4 Development and elution of column

In order to prepare slurry for column chromatography, the extracted viscous mass after dissolving in little methanol was mixed with silica gel (60-120), used for column chromatography to completely adsorb the viscous mass on silica gel. The slurry prepared was than dried in air and free flowing granules were obtained. The dried slurry was later packed over a silica gel glass column packed in petroleum ether.

Non-absorbent cotton was used to plug the lower end of the glass column and a small filter paper was placed over it. The glass column was than filled with petroleum ether as solvent and than silica gel (60-120) was slowly added allowing the silica gel to settle down up to the required length of the column. The column was then allowed to run several times with petroleum ether in order to remove air bubbles. The slurry prepared earlier was than packed over this column and run successively by various solvents in increasing order of polarity. the column was developed by running a combination of series of solvent in different combinations of petroleum ether (100 v/v), petroleum ether with $CHCl_3$ with gradual increase in $CHCl_3$ content (75:25, 50:50, 50:75v/v) only chloroform (100 v/v), and later ratios of chloroform/methanol (99:1,99:2,99:5,99/10 v/v). Pre coated TLC plates were used to analyze eluents. The fraction showing same R_f values in TLC were combined and recrystallised to obtain pure phytoconstituents.

2.5 *In vitro* α-glucosidase inhibition assay

The ethanolic, chloroform, and petroleum ether fractions of *P. acidus* along with isolated compounds were subjected to enzyme inhibition assay along with reference compound acarbose at a dose range of 30-500 µg/ml following the method by (Dong *et al*. 2012) with few modifications. All sample solutions and standard acarbose were prepared in DMSO and 60 µl of the same was taken along with 50 µl phosphate buffer (0.1 M, at pH 6.8) and 0.2 U/ml of α-glucosidase solution was placed in an incubator for 20 min at 37°C in 96 well plate. Following incubation, *p*-nitrophenyl-α-D-glucopyranoside (PNPG) (50 µl, 5 mM solution prepared in in 0.1 M phosphate buffer) was put into all the wells and further placed in an incubator at 37°C for 20 min. The reaction was halted by addition of 160 µl of 0.2 M Na_2CO_3 into each well. The absorbance (A) at 405 nm was recorded by micro-plate reader. The control consisted of 60 µl buffer solutions only. For blank readings the phosphate buffer replaced the enzyme solution and absorbance was observed.

The α-glucosidase inhibition action was indicated as percent inhibition and calculated by using following formula:

$$\% \text{ Inhibition} = \frac{A_0 - A_{sample}}{A_0} \times 100$$

where, A_o, A_{sample} represents absorbance of 100% enzyme action and drug with the enzyme, respectively. The IC_{50} values are taken to indicate 50% enzyme inhibiting activity of the drug fractions.

3. Results

3.1 Characterisation of isolated compounds

The structure of the isolated compounds was elucidated with the help of UV-VIS spectrophotometer, FTIR, ESI-MS, MS, ^{1}H-NMR, ^{13}C-NMR. Herein, we report spectroscopic data as shown below.

n-Docosane, $C_{22}H_{46}$ (PA-1)

Elution of the chromatographic column with petroleum ether (PE)-chloroform (3:1) gave colorless crystals of PA-1, which were recrystallized from chloroform, 900 mg (0.8%). R_f: 0.23(PE /$CHCl_3$, 3:1v/v) ,m.p 43-45°C, UV l_{max}(MeOH): 280nm, IRn_{max}(CCl_4): 2915,2848,1402,762 cm^{-1}, ^{1}H NMR ($CDCl_3$): d 0.88(6H, t, J=8Hz Me-1 and Me-22), d 1.21 (2H, s, CH2), d1.25 (36H, brs, 18x CH_2), d1.30 (2H, s, CH_2), ^{13}C NMR ($CDCl_3$): d 32.23 (CH_2), d 30.01(18x CH_2), d22.98 (CH_2), d14.35 (CH_3-1 and CH_3-26), HRMS: m/z: $[M]^+$ 310.

Compound PA-1, an aliphatic hydrocarbon, was procured as colourless crystals from a mixture of solvents petroleum ether and chloroform in the ratio 3:1. It did not react with tetra nitro methane and bromine water indicating that compound isolated was a saturated hydrocarbon.

Its IR spectra exhibited the existence of long aliphatic chain at 762.52 cm^{-1}.

The ^{1}H NMR spectra of PA-1 exhibited two three proton triplets at δ0.88 corresponding to Me-1 and Me-22. The λ1.25 showed the presence of 20 × CH_2 integrating to 40 protons. (Figure 1)

^{13}C NMR showed δ_c14.35 corresponding to terminal carbon atoms (Me-1, Me-22). Other carbon atoms resonated at δ32.23, 30.01, and 22.98, respectively (Figure 2).

On the basis of HRMS data, the molecular weight was stated as 310 in accordance with the molecular formula $C_{22}H_{46}$. The PA-1 mass spectrum showed C_nH_{2n+1}, C_nH_{2n} and C_nH_{2n-1} ion with a difference of 14 mass unit and reducing in abundance with a increasing molecular weight of long chain hydrocarbon, *i.e.,* m/z [M] 310, [M-H] 309, [M-H-CH_2] 295,281,267 (Figure 3).On the basis of the following information, the structure of PA-1 was proposed as n-Docosane.

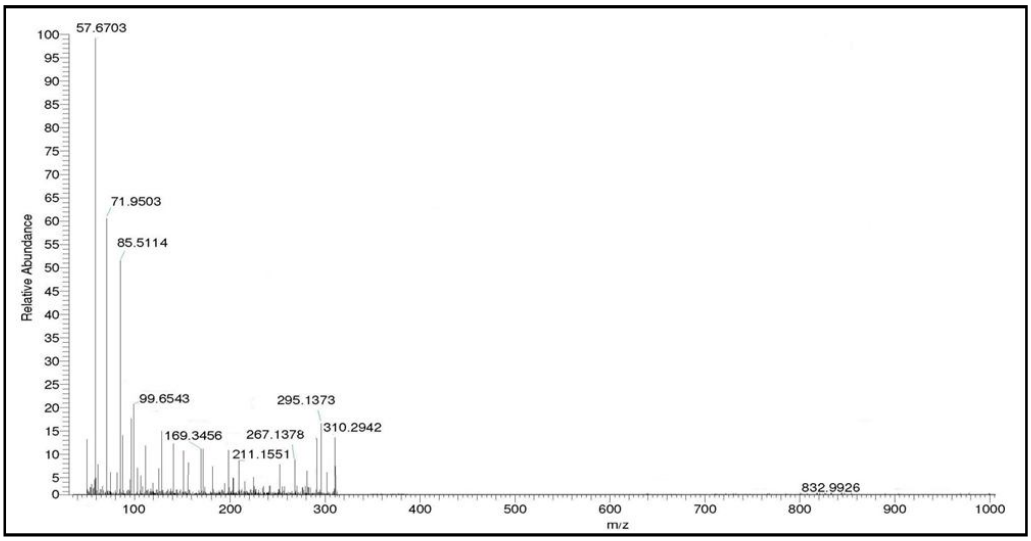

Figure 1: HRMS spectrum of PA-1.

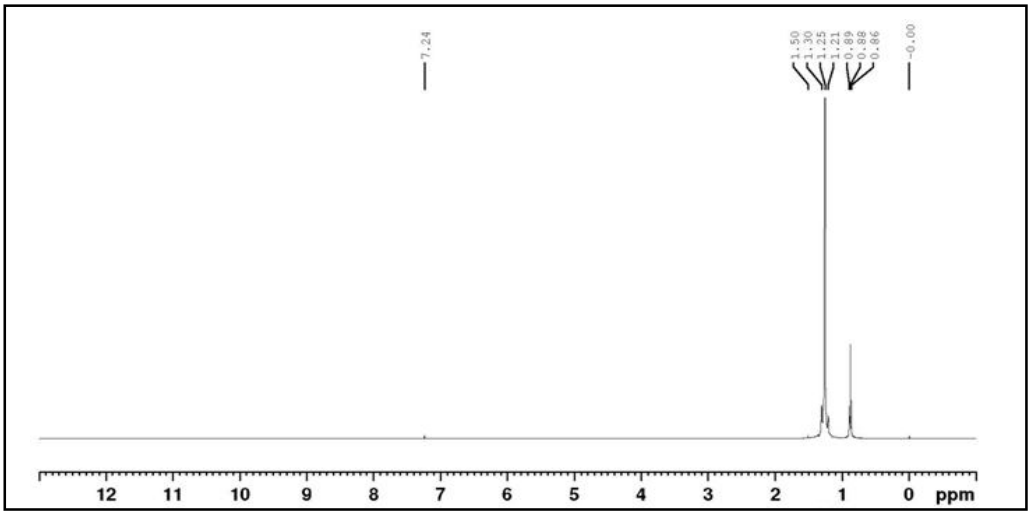

Figure 2: ^{1}H NMR spectrum of PA-1.

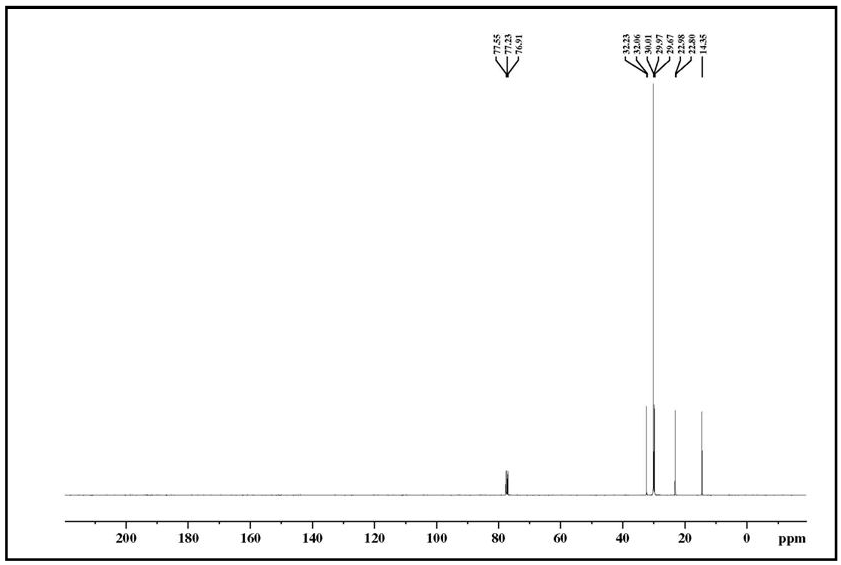

Figure 3: ^{13}C NMR spectrum of PA-1.

Table 1: ^{13}C NMR and ^{1}H NMR spectral data for PA-2 in $CDCl_3$ (400MHz)

Carbon No.	^{13}C NMR (δ)	^{1}H NMR (δ)	Carbon No.	^{13}C NMR (δ)	^{1}H NMR (δ)
C-1	37.76	1.32m	**C-16**	28.16	1.94
C-2	31.69	1.99m	**C-17**	56.07	1.17
C-3	70.65	3.19 (m,H-3α)	**C-18**	11.95	0.41(s,Me-18)
C-4	41.89	2.93	**C-19**	19.46	0.73(s,Me-19)
C-5	140.79	-	**C-20**	36.11	1.54
C-6	120.75	5.38 (s,1H)	**C-21**	18.71	0.67(d,J=8.0 MHz)
C-7	31.69	1.56m	**C-22**	33.50	1.30
C-8	31.94	1.76	**C-23**	25.68	1.57
C-9	49.73	0.92m	**C-24**	45.36	1.17
C-10	36.69	-	**C-25**	29.88	1.94
C-11	20.84	0.99	**C-26**	19.85	0.56 (d, J=8.0 MHz)
C-12	39.71	1.20	**C-27**	19.03	0.60 (d, J=8.0 MHz)
C-13	42.16	1.23	**C-28**	23.89	1.73
C-14	56.34	1.27	**C-29**	15.01	0.90
C-15	25.68	1.20			

β-sitosterol, $C_{29}H_{50}O$ (PA-2)

Elution of chromatographic column with PE-$CHCl_3$ (1:1) mixture provided colourless needles of PA-2, that were recrystallised from ethanol, 900 mg (0.26% yield), R_f: 0.31 ($CHCl_3$), m.p - 132-133°C, UV λ_{max}(MeOH): 220 nm IRn_{max}(CCl_4): 3785, 3407, 2954, 1658, 1463, 1241, 1191, 880, 760, 625 cm^{-1}, ^{1}H NMR($CDCl_3$) (Table 1), ^{13}C NMR ($CDCl_3$): (Table 1), HRMS: m/z: 414 $[M]^+$, 396[M-H_2O], 381[M-H_2O-CH_3], 273,255,199,173,159.

Compound PA-2, a sterol was procured as a colourless amorphous white powder from petroleum ether: $CHCl_3$ (1:1) eluants. It gave positive Liebermann-Buchard reaction for steroids. Its IR spectra showed absorption bands for hydroxyl group (3407 cm^{-1}) and also for unsaturation (1658 cm^{-1}). The HRMS showed molecular ion peak at m/z 414 correlating to a steroid $C_{29}H_{50}O$. It suggested five double bond equivalents; four of which were included in the steroidal structure and one in the olefinic linkage. The other characteristic peaks observed at m/z 414 $[M]^+$, 396[M-H_2O]$^+$, 381, 273 [M-side chain, $C_{10}H_{21}]^+$, 255[273-H_2O]$^+$, 213[255- fission of ring D]$^+$ and 198 [213-Me]. These fragmentations indicated that the molecule is a C_{29}- sterol molecule having one double bond in the steroidal carbon skeleton, hydroxyl group at C-3 in ring A and suggesting the presence of the olefinic linkage in ring B at C-5 and which was allocated on the basis of biogenetic considerations. The mass spectrum showed the presence of ethyl molecule in the side chain that was indicated at C-24 on the basis of biological consideration (Figure 4). The ^{1}H NMR analysis of PA-2 showed at δ5.05, a one proton singlet ascribed to C-6 olefenic proton. A broad multiplet of one proton at δ3.19 suggested the

existence of 3α-methine proton (axial) interacting with C-2 axial, C-2 equatorial, and C-4 equatorial protons. Three doublets at δ 0.67 (J=8.0 Hz), 0.56 (J=8.0 Hz), 0.60 (J=8.0 Hz) and 0.82; integrating three protons each, were assigned to carbon atoms corresponding to C-21, C-26, C-27 protons of secondary methyl groups. The remaining two tertiary C-18 and C-19 methyl proton signals showed as singlet at δ 0.41 and 0.73, respectively. Appearance of all the methyl signals in the range of δ 0.4-0.83, indicated that methyl groups were joined to saturated carbon atom. The remaining, methylene and methane protons resonated in the region of δ 1.99-1.17. Beside this, a broad signal at δ 2.95 of the anomeric C-1 proton was present. (Table 1) (Figure 5). Additional proof regarding the structure of PA-2 was given by the ^{13}C NMR spectral information that indicated the molecule had 29 carbon atoms in it. Signals at δ 140.79 and 120.75 were linked to C-5, C-6 unsaturated carbons and at δ 70.65 to C-3 carbinol carbon. The signals at δ 11.95 ppm and 19.46 ppm are assignable to the methyl carbons of C19 and C18 respectively (Figure 6) The distinguishing chemical shift values (Table 1) in NMR spectra are very similar to data documented in the literature for β-sitosterol (Patra *et al*., 2010; Greca *et al.*, 1990).

Based on ^{1}H NMR, ^{13}C NMR, the molecular formula of the isolated compound was proposed as $C_{29}H_{50}O$. On the basis of these findings, the structure of PA-2 has been established as β-sitosterol.

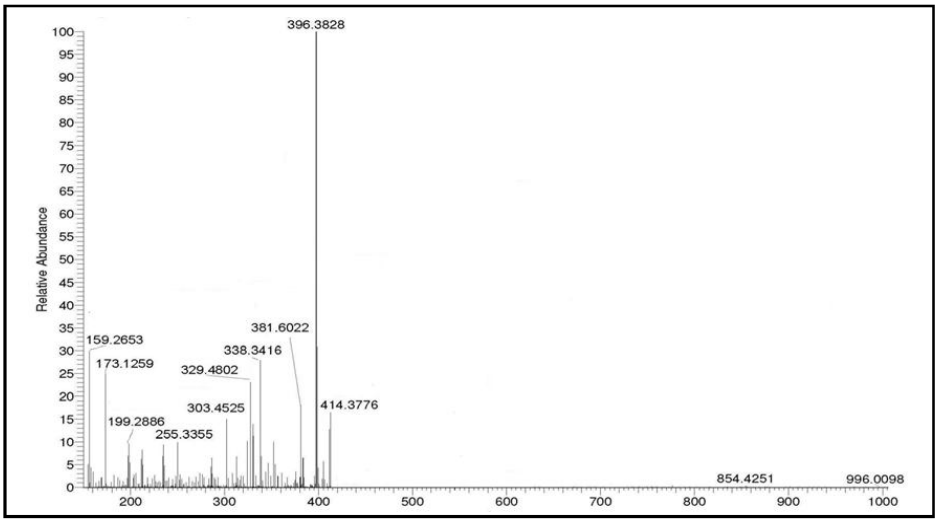

Figure 4: HRMS spectrum of PA-2.

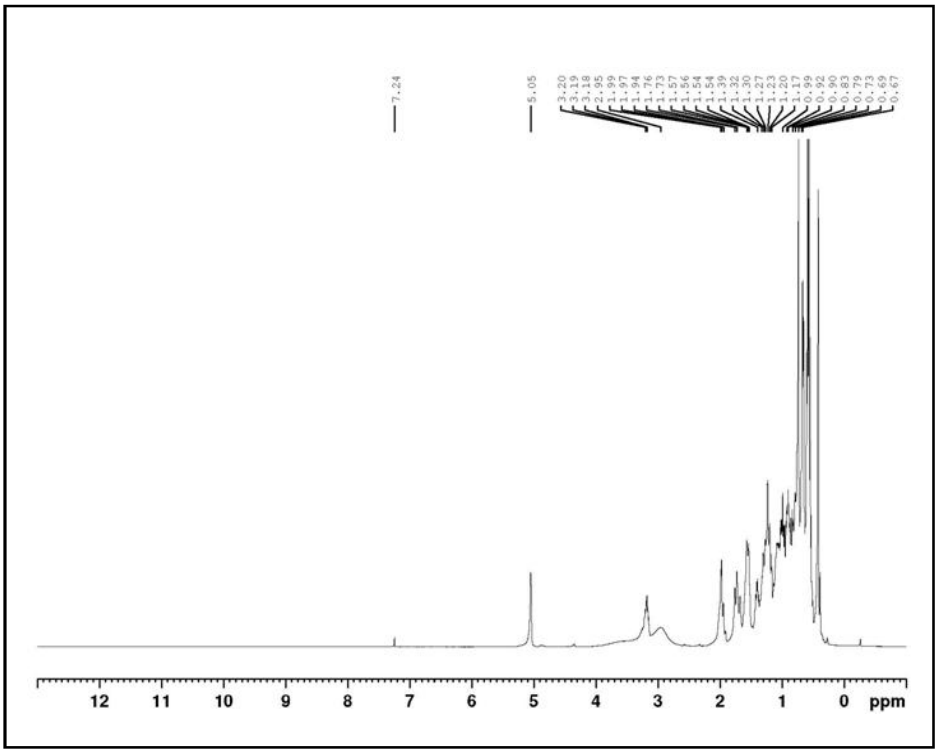

Figure 5: ^{1}H NMR spectrum of PA-2.

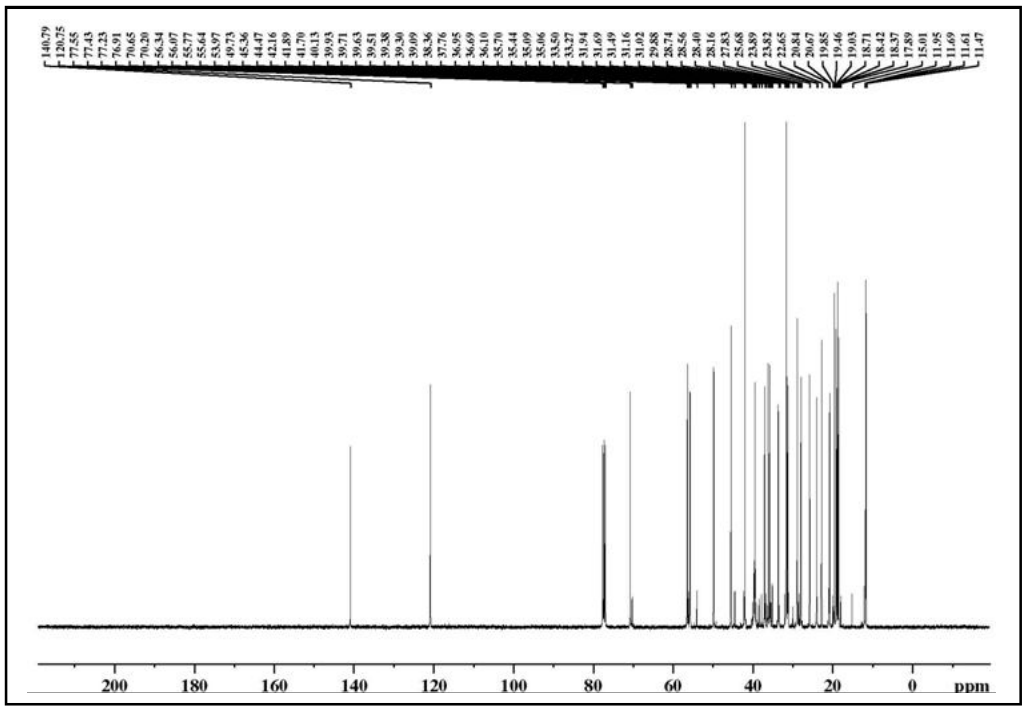

Figure 6: ^{13}C NMR spectrum of PA-2.

Table 2: ^{13}C NMR and ^{1}H NMR spectral data for PA-3 in $CDCl_3$ (400MHz)

Carbon atoms	^{13}C NMR	^{1}H NMR	Carbon atoms	^{13}C NMR	^{1}H NMR
C-1	38.72		**C-16**	35.60	
C-2	27.43		**C-17**	43.01	
C-3	79.01	3.19(1H, dd, J=8	**C-18**	47.99	
C-4	38.87	Hz, 4 Hz,H-3a)	**C-19**	48.32	2.32-2.39 (1H, dt, J = 8.0 and 20 Hz, H-19)
C-5	55.31		**C-20**	150.98	
C-6	18.33		**C-21**	29.86	
C-7	34.30		**C-22**	40.01	
C-8	40.85		**C-23**	28.00	1.01 (3H, brs,Me-23)
C-9	50.46		**C-24**	15.37	0.95 (3H, brs,Me-24)
C-10	37.18		**C-25**	16.12	0.74 (3H, brs,Me-25)
C-11	20.94		**C-26**	15.99	0.92 (3H, brs,Me-26)
C-12	25.16		**C-27**	14.56	0.81 (3H, brs,Me-27)
C-13	38.07		**C-28**	18.01	0.77 (3H,brs,Me-28)
C-14	42.84		C-29	109.32	4.67 (1H,brs,H_2-29a), 4.55(1H,brs,H_2-29b)
C-15	27.43		**C-30**	19.32	1.66 (3H,brs,Me-30)

3β-hydroxylup-20(29)-ene- lupeol, $C_{30}H_{50}O$ (PA-3)

Elution of column with petroleum ether-chloroform (1:3) mixture furnished white microcrystalline powder of PA-3, recrystallised from ethanol, 20 mg (0.006% yield) R_f: 0.35, $CHCl_3$/EtOAc 9:1 v/v, m.p 213.0°C, UV_{max}(MeOH): 228, 285 nm, IRn_{max}(CCl_4): 3295, 2926,1725, 1643, 1454, 1381, 1031, 761 cm^{-1}, HRMS m/z: 425 [M+ - H], 409, [M+ - OH] 218, 207, and 189. ^{1}H NMR and ^{13}C NMR(Table 2).

PA-3 gave positive reaction to Liebermann-Burchard test. The IR spectra showed diagnostic absorption bands for presence of hydroxyl group (3295 cm^{-1}) and for unsaturation (1643 cm^{-1}) (Figure 8). The HRMS showed a molecular ion peak at m/z 426 correlating to molecular formula ($C_{30}H_{50}O$). It showed six double bond equivalents; five of them were added in the five membered carbon framework of the triterpenic molecule and one in the vinylic linkage. The distinguished

ion peaks generated at m/z 411 [M-CH_3]$^+$, 383[411-C_2H_4],207[383-$C_{13}H_{22}$],189[207-H_2O] suggested the saturated nature of the hydroxyl group in ring A, which was situated at C-3 on the basis of biogenetic analogy (Figure 7).

The ^{1}H NMR spectra of PA-3 exhibited two, broad signals at δ 4.67 and δ 4.55 of one proton each, which were assigned to methylene 29-a and 29-β protons, respectively. Double doublet at δ 3.19 of one proton with coupling interactions of 8.0 and 4.0 Hz was assigned to 3α-methine proton. Signals attributed to seven tertiary methyl groups, which are also a reflection of a lupeol-type triterpene. The seven broad singlets, integrating three protons each, at δ 1.66, δ 1.01, δ 0.95, δ 0.74, δ 0.92, δ 0.81, δ 0.77 were due to methyl protons of C-30, C-23, C-24, C-25, C-26, C-27 ,and C-28. The deshielding methyl signals at δ 1.66 indicated that C-30 methyl functionality was located on the vinylic carbon (Figure 8).

Additional proof regarding the structure of PA-3 was derived from its ^{13}CNMR spectral data which indicated the presence of thirty carbon atoms in the compound. The signals at δ 150.1, 109.32, and 79.01 were attributed to s C-20, C-29 unsaturated carbons, and C-3 carbinol carbons, simultaneously (Figure 9).

The structure of PA-3 has been formulated as lup-20(29) en-3β-ol, a known pentacyclic triterpene on the basis of spectral analysis.

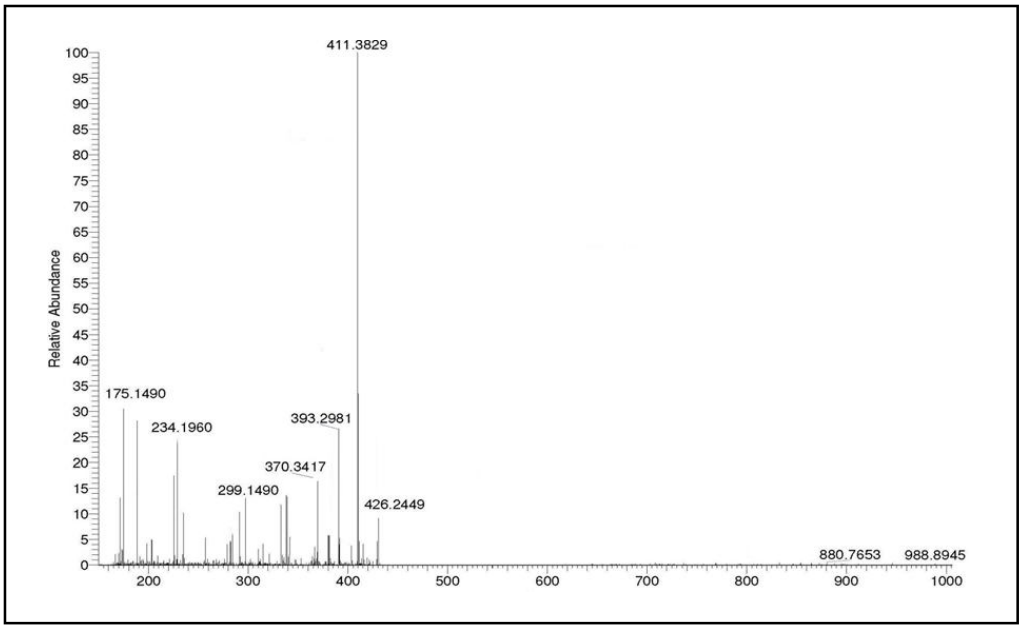

Figure 7: HRMS spectrum of PA-3.

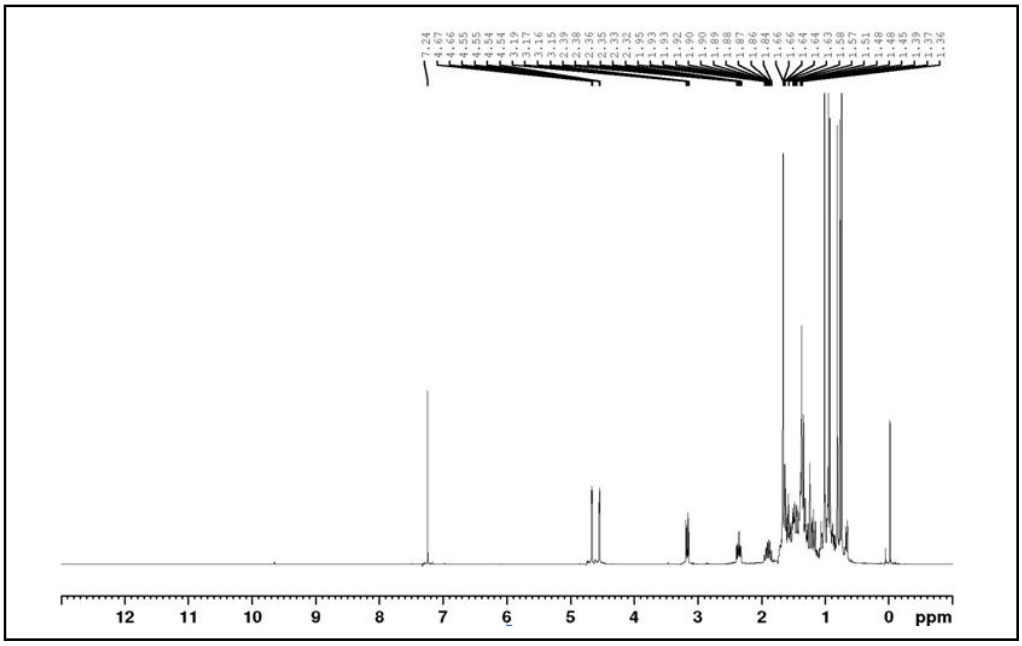

Figure 8: ^{1}H NMR spectrum of PA-3.

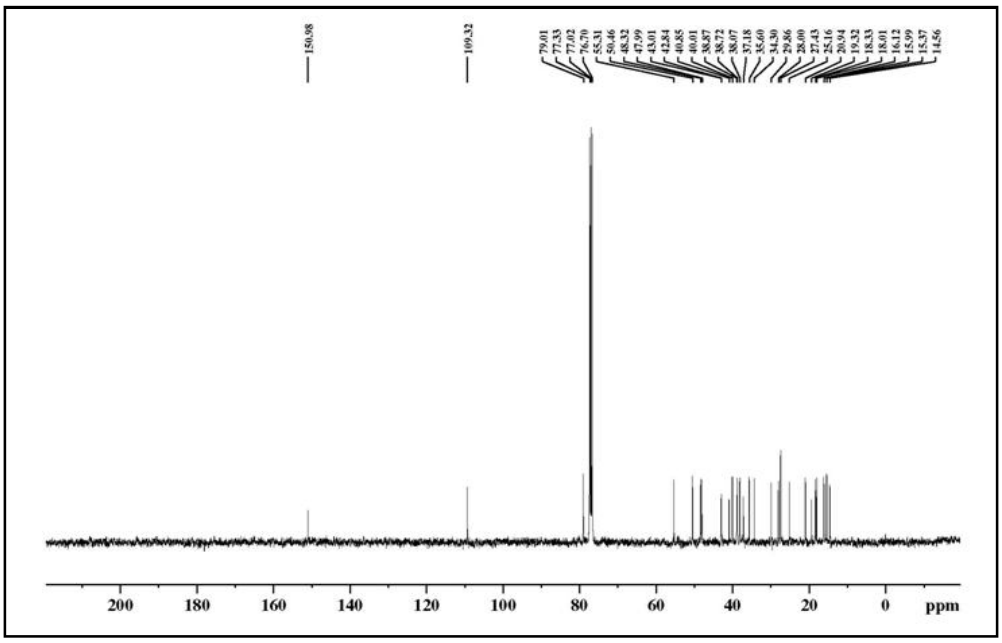

Figure 9: ^{13}CNMR spectrum of PA-3.

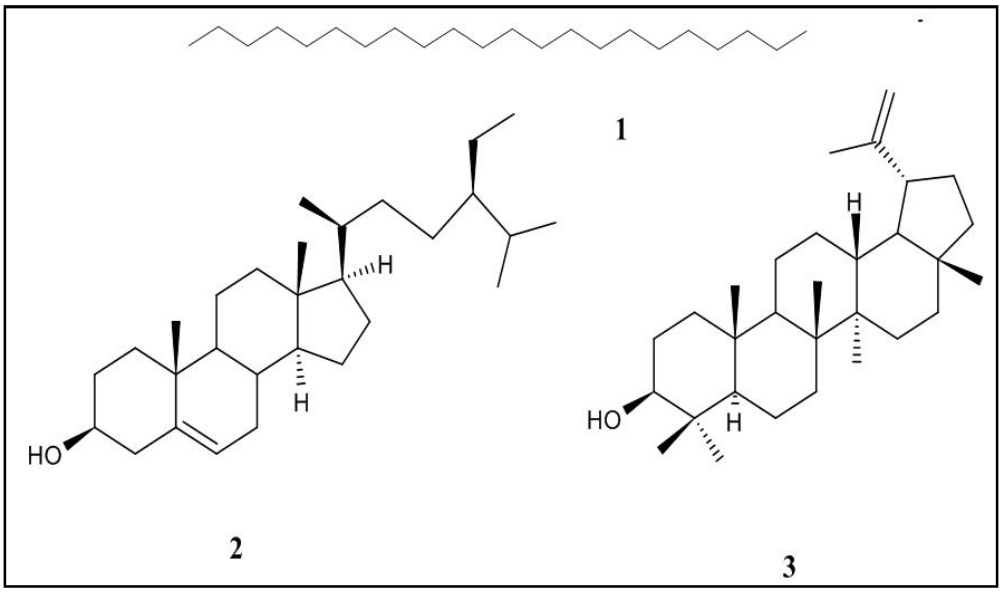

Figure 10: Chemical structures of isolated compounds 1) PA-1 2) PA-2 3) PA-3.

3.2 *In vitro* α-glucosidase inhibition assay of *P. acidus*

In order to explore potential α-glycosidase inhibitors, various fractions and all of the isolated compounds were evaluated for α-glycosidase inhibitor activity. As shown in Figure 10, there was significant variation in the inhibitory activity among the fractions as well as the isolated phytoconstituents. Inhibition by *P. acidus* petroleum ether fraction, chloroform fraction and ethanolic fraction occurred in a concentration-dependent method, and chloroform fraction showed enzyme inhibition (IC_{50} value 67.45 µg/mL) more than that of ethanolic (IC_{50} value 69.72 µg/ml) and petroleum ether fraction (IC_{50} value 98.21 µg/ml). Among the isolated compounds PA-1 showed no inhibition while compound PA-2 (IC_{50} value 58.57 µg/ml) and PA-3 (IC_{50} value 53.35 µg/ml) exhibited maximum activity compared to acarbose (IC_{50} value 41.23 µg/ml) as indicated in Table 3. The data showed that semi-polar fraction exhibited more inhibition activity which can be correlated to the isolated compounds PE-2 and PE-3 which were isolated from chloroform fraction of the column chromatography. This finding is in correlation of reported data of inhibitory effect of β-sitosterol (PE-2) and lupeol (PA-3) (Yuca *et al.,* 2022). This *in vitro* finding indicated the chloroform extract of *P. acidus* lowers the post parandial glucose levels due to inhibition of α-glycosidase, an enzyme responsible for absorption of monosaccharides present in the food.

Table 3: ***In vitro*** **α-glucosidase inhibitory activity of fractions and isolated compounds of** ***P. acidus***

Conc.(µ/ml)	Percent inhibition					
	Acarbose	PE fraction	$CHCl_3$ fraction	EtOH fraction	PA-2	PA-3
20	38.2 ± 0.41	11.83 ± 0.47	15.25 ± 0.67	14.65 ± 1.20	28.35 ± 0.17	33.45 ± 0.87
40	54.6 ± 0.88	20.26 ± 0.84	30.65 ± 1.39	28.42 ± 0.64	39.42 ± 0.35	40.32 ± 0.66
60	75.25 ± 0.78	28.93 ± 0.98	44.93 ± 1.42	43.81 ± 0.89	54.65 ± 0.68	57.23 ± 1.95
80	87.64 ± 1.50	35.63 ± 1.32	59.47 ± 0.74	50.56 ± 0.14	66.75 ± 1.04	68.32 ± 0.71
100	98.32 ± 1.53	42.73 ± 0.54	70.53 ± 0.12	69.45 ± 0.69	72.52 ± 1.28	79.62 ± 0.34
IC_{50}	**41.23**	**98.21**	**67.45**	**69.72**	**58.57**	**53.35**

Data expressed as mean ± SEM, n= 3; IC_{50} = conc. for 50% inhibition

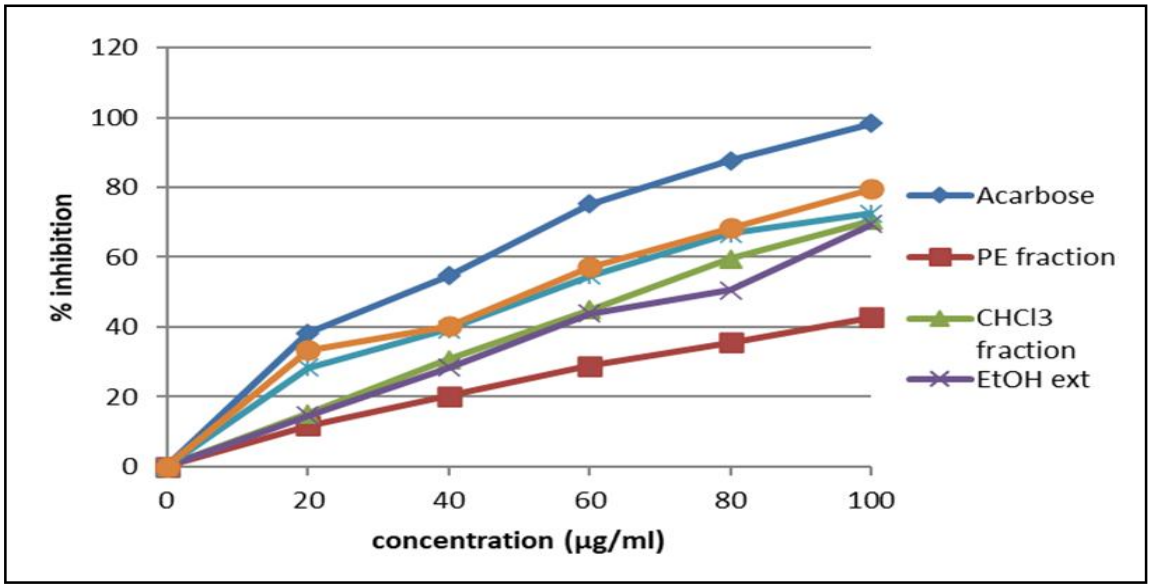

Figure 10: ***In vitro*** **α-glucosidase inhibition by ethanol extract, petroleum ether fraction and chloroform fraction and isolated compounds PA-2, PA-3 of** ***P. acidus vs*** **acarbose.**

4. Discussion

Numerous studies demonstrated that phenolic compounds in food and nutraceutical sources are given attention due to their biological properties such as glucosidase inhibition activities. Detail chemical analysis of stem bark of *P. acidus* furnished the isolation of three chemical compounds, namely n-docosane ($C_{22}H_{46}$), β-sitosterol ($C_{29}H_{50}O$), and lup-20 (29) en-3β-ol ($C_{30}H_{50}O$). The high phenolic and flavonoid content of chloroform extract from which these compounds have been isolated indicate that the pharmacological potential shown by this plant may be because of some of these sesquiterpenoids and terpenoids constituents. Though, previously known these compounds have been isolated from stem bark of *P. acidus* for the first time. Among these compounds, n-docosane has been reported for the first time from *P. acidus.*

Various approaches such as dietary restrictions or/and drug treatments has been put forth to modify the pathways for carbohydrate metabolism for diabetes therapy (Ghalib and Mehrotra, 2022, Hashim *et al.*, 2023). Phytosterols such as betasterol are plant metabolites with various health benefits like lowering of blood cholesterol and LDL one of the causes of diabetes (Tiwari *et al.,* 2022)

The results of α-glucosidase inhibitory assay of *P. acidus* and isolated compounds exhibited a dose related supression of α-glucosidase that was analogous to acarbose (IC_{50} 41.23 µg/ml). The utmost α-glucosidase supression was accomplished with compound PA-2 (IC_{50} 53.35 µg/ml), followed by PA-2 (IC_{50} 58.57 µg/ml) while PA-1 did not show any inhibition activity. Chloroform fraction of the extract showed more inhibition (IC_{50} 67.45 µg/ml) as compared to ethanol extract (IC_{50} 69.72 µg/ml) and petroleum ether fraction (IC_{50} 98.21 µg/ml) when compared to standard drug acarbose (IC_{50} 41.23 µg/ml). The data showed that semi-polar fraction exhibited more inhibition activity which can be correlated to the isolated compounds PE-2 and PE-3 which were isolated from chloroform fraction of the column chromatography. This finding is in correlation of reported data of inhibitory effect of β-sitosterol (PE-2) and lupeol (PA-3) (Yuca *et al.,* 2022). Docosane although did not show α-glucosidase inhibition, it has been used in organic synthesis and has been found to possess antimicrobial property (Karabay Yavasoglu *et al.,* 2007). This *in vitro* finding indicated the chloroform extract of *P. acidus* lowers the post parandial glucose levels due to inhibition of α-glycosidase, an enzyme responsible for absorption of monosaccharide's present in the food. These results suggest that *P.*

acidus stem bark may be utilized as an effective source of α-glucosidase inhibition for pharmaceutical uses. Further research is still needed to investigate the phytochemical and various biological effects in this species.

5. Conclusion

In order to scientifically justify the therapeutic claims of *P. acidus* for the cure of various ailments both in folklore and traditional system of medicine, and to investigate the phytoconstituents present in these plants that may be responsible for these therapeutic activities. The methanolic extract of both the plants were subjected to separation using preparative chromatographic technique. The chloroform fractions eluted an alkane and two terpenoid compounds. It can be deduced from the *in vivo* antidiabetic activity exhibited by fractions and isolated compounds that the chloroform fraction of *P. acidus* can be safely employed as an alternate therapy to control diabetes related conditions and also validates its ethnopharmacological use as antidiabetic. Furthermore, detailed pharmacological evaluations are needed to demonstrate the exact mechanism involve for the antidiabetic activity.

Acknowledgements

The authors extend their sincere appreciation to the Honourable Chancellor of Integral University, Lucknow-226026, Uttar Pradesh, India, for generously providing research infrastructure. They also express their gratitude to the Dean, Faculty of Pharmacy at Integral University for providing the essential resources. Special thanks are extended to the R&D cell at Integral University for assigning the Manuscript Communication Number IU/R&D/2024-MCN0002484.

Conflict of interest

The authors declare no conflicts of interest relevant to this article.

References

American Diabetes Association, (2014). Standards of medical care in diabetes 2014. Diabetes Care, **37**(Supplement 1):S14-S80.

Ajmal, M.; Badruddeen; Ahmad,M.; Akhtar, J and Alam, M.A. (2023). Addressing potential pharmacological adverse reactions when taking dapagliflozin for the management of type 2 diabetes: A case report. Ann. Phytomed., **12**(2):402-405.

Asghari, A. A.; Hosseini, M.; Bafadam, S.; Rakhshandeh, H.; Farazandeh, M and Mahmoudabady, M (2022). *Olea europaea* L.(olive) leaf extract ameliorates learning and memory deficits in streptozotocin-induced diabetic rats. Avicenna Journal of Phytomedicine, **12**(2):163.

Aslan, M.; Orhan, N.; Orhan, D. D and Ergun, F. (2010). Hypoglycemic activity and antioxidant potential of some medicinal plants traditionally used in Turkey for diabetes. Journal of Ethnopharmacology, **128**(2): 384-389.

Della, G. M.; Monaco, P and Previtera, L. (1990). Stigmasterols from *Typha latifolia*. Journal of Natural Products, **53**(6):1430-1435.

Dong, H. Q.; Li, M., Zhu, F.; Liu, F. Land Huang, J. B. (2012). Inhibitory potential of trilobatin from *Lithocarpus polystachyus* Rehd against α-glucosidase and α-amylase linked to type 2 diabetes. Food Chemistry, **130**(2):261-266

Duraisami, R.; Sengottuvelu, S.; Prabha, T.; Sabbani, S.; Presenna, D.S and Muralitharan, C.K. (2021). Evaluation of antidiabetic efficacy potency of polyherbal formulations in experimentally induced hyperglycemic rats. Ann. Phytomed., **10**(2):286-291.

Gao, H. and Kawabata, J. (2008). 2-Aminoresorcinol is a potent α-glucosidase inhibitor. Bioorganic and Medicinal Chemistry Letters, **1**(2):812-815.

Ghalib, R and Mehrotra, N. (2022). *In vitr*o α-glucosidase inhibitory activity of nanoencapsulated *Cuminum cyminum* L. (Angiosperms: Apiaceae) and it's interaction with acarbose. Ann. Phytomed., **11**(1):465-471.

Hardie, D. G. (2017). Targeting an energy sensor to treat diabetes. Science, **357**(6350):455-456.

Hashim, M.; Badruddeen; Akhtar, J.; Ahmad, M.; Islam, A.; Ahmad, A and Zahra, F. (2023). Diabetic nephropathy: An outline on molecular mechanism and protective pathways of phytoconstituents. J. Phytonanotech. Pharmaceut. Sci., **3**(3):1-16.

Hazarika, R.; Abujam, S. S and Neog, B. (2012). Ethno medicinal studies of common plants of Assam and Manipur. Int. J. Pharm. Biol. Arch., **3**(4):809-815.

Karabay Yavasoglu, N. U.; Sukatar, A.; Ozdemir, G and Horzum, Z. (2007). Antimicrobial activity of volatile components and various extracts of the red alga *Jania rubens*. Phytotherapy Research: An International Journal Devoted to Pharmacological and Toxicological Evaluation of Natural Product Derivatives, **21**(2):153-156.

Kirtikar, K. R. (1991). Indian Medicinal Plants. (No Title):1158-1159

Kumari, N.;Akhtar, J.; Badruddeen; Khan, M. I and Ahmad, M. (2023). Formulation development and *in vivo* evaluation of nanoemulgel containing *Adhatoda vasaka* (L.) Nees extract for wound healing activity. Ann. Phytomed., **12**(2):720-729.

Lebovitz, H. E. (2001). Effect of the postprandial state on nontraditional risk factors. The American Journal of Cardiology, **88**(6):20-25.

Lemmens, R. H. M. J. (1999). Medicinal and poisonous plants. Backhuys Publishers. pp:45-48

Liu, C. T.; Sheen, L. Y and Lii, C. K. (2007). Does garlic have a role as an antidiabetic agent?. Molecular nutrition and Food Research, **51**(11): 1353-1364.

Marcovecchio, M. L.; Lucantoni, M and Chiarelli, F. (2011). Role of chronic and acute hyperglycemia in the development of diabetes complications. Diabetes Technology and Therapeutics, **13**(3):389-394.

Mehta, A.; Zitzmann, N.; Rudd, P. M.; Block, T. M and Dwek, R. A. (1998). α-glucosidase inhibitors as potential broad based antiviral agents. FEBS Letters, **430**(1-2):17-22.

Morton, J. (1987). Guava fruits of warm climates. Julia F. Morton, Miami, FL: 356-363.

Ogurtsova, K.; da Rocha Fernandes, J. D.; Huang, Y.; Linnenkamp, U.; Guariguata, L.; Cho, N. H and Makaroff, L. E. (2017). IDF Diabetes Atlas: Global estimates for the prevalence of diabetes for 2015 and 2040. Diabetes Research and Clinical Practice, **128**:40-50.

Palai, S.; Patra, R.; Jena, S.; Nikunj, M.; Sardar, K.K and Parija. S.S. (2023). A comprehensive review on potential benefit *Annona squamosa* L. leaves for the treatment of diabetic wounds. Ann. Phytomed., **12**(2):149-160.

Patra, A. K and Saxena, J. (2010). A new perspective on the use of plant secondary metabolites to inhibit methanogenesis in the rumen. Phytochemistry, **71**(11-12):1198-1222.

Rizk, A. F. M. (1987). The chemical constituents and economic plants of the Euphorbiaceae. Botanical Journal of the Linnean Society, **94**(1-2):293-326.

Sabiu, S.; O'neill, F. H and Ashafa, A. O. T. (2016). Kinetics of α-amylase and α-glucosidase inhibitory potential of *Zea mays* Linnaeus (Poaceae), *Stigma maydis* aqueous extract: An *in vitro* assessment. Journal of Ethnopharmacology, **183**:1-8.

Seo, W. D.; Kim, J. H.; Kang, J. E.; Ryu, H. W.; Curtis-Long, M. J.; Lee, H. S and Park, K. H. (2005). Sulfonamide chalcone as a new class of α-glucosidase inhibitors. Bioorganic and Medicinal Chemistry Letters, **15**(24): 5514-5516.

Siddiqui, Z.; Khan, M. I.; Akhtar, J and Ahmad, M. (2022). Multifunctional role of *Phyllanthus acidus* L. As a therapeutic agent for management of diabetes and associated complications: A review. Biomedical and Pharmacology Journal, **1**(4):1821-1831.

Siddiqui, Z.; Khan, M. I.; Akhtar, J and Ahmed, M. (2023). *In vitro* antioxidant activity, pharmacognostical evaluation, HPTLC and FTIR fingerprinting of *Phyllanthus acidus* L. stem bark extract for better application in phytotherapy. Biomedical and Pharmacology Journal, **16**(3): 1381-1393.

Singh,R.P.; Goswami, S and Pathak, S. (2023). HPTLC fingerprinting of quercetin and assessment of *in vitro* and *in vivo* antihyperglycemic effect of the leaves of *Tagetes erecta* L.. Ann. Phytomed.,**12**(2):562-571.

Tan, S. P.; Tan, E. N. Y.; Lim, Q. Y and Nafiah, M. A. (2020). *Phyllanthus acidus* (L.) Skeels: A review of its traditional uses, phytochemistry, and pharmacological properties. Journal of Ethnopharmacology, **253**: 112610.

Tiwari, P.; Ahamad, V.; Ansari, T.M and Ahsan, F. (2022). Augumentation and evaluation of betasitosterol based liposomes. Ann. Phytomed., **11**(1):648-656.

Toeller, M. (1994). α-glucosidase inhibitors in diabetes: Efficacy in NIDDM subjects. European Journal of Clinical Investigation, **24**(3):31-35.

Unander, D. W.; Webster, G. L and Blumberg, B. S. (1990). Records of usage or assays in Phyllanthus (Euphorbiaceae) I. subgenera Isocladus, Kirganelia, Cicca and Emblica. Journal of Ethnopharmacology, **30**(3):233-264.

Yee, H. S and Fong, N. T. (1996). A review of the safety and efficacy of acarbose in diabetes mellitus. Pharmacotherapy: The Journal of Human Pharmacology and Drug Therapy, **16**(5):792-805.

Yuca, H.; Özbek, H.; Demirezer, L. Ö and Güvenalp, Z. (2022). Assessment of the α-glucosidase and α-amylase inhibitory potential of *Paliurus spina-christi* Mill. and its terpenic compounds. Medicinal Chemistry Research, **31**(8):1393-1399.

Zhou, B.; Lu, Y.; Hajifathalian, K.; Bentham, J.; Di Cesare, M.; Ezzati, M and NCD Risk Factor Collaboration. (2016). Worldwide trends in diabetes since 1980: A pooled analysis of 751 population-based studies with 4.4 million participants. The Lancet, **387**(10027):1513-1530.

Zitzmann, N.; Mehta, A. S.; Carrouée, S.; Butters, T. D.; Platt, F. M.; McCauley, J and Block, T. M. (1999). Imino sugars inhibit the formation and secretion of bovine viral diarrhea virus, a pestivirus model of hepatitis C virus: Implications for the development of broad spectrum anti-hepatitis virus agents. Proceedings of the National Academy of Sciences, **96**(21):11878-11882.

Citation **Zeba Siddiqui, Mohammad Irfan Khan, Badruddeen, Juber Akhtar, Mohammad Ahmad, Manvi and Gayyur Fatima (2024). Isolation and characterization of a-glucosidase inhibitors from *Phyllanthus acidus* (L.) Skeels stem bark . Ann. Phytomed., 13(1):1100-1110. http://dx.doi.org/10.54085/ap.2024.13.1.118.**